

# Shallow-water seismoacoustic noise generated by tropical storms Ernesto and Florence

James Traer, Peter Gerstoft, Peter D. Bromirski,  
William S. Hodgkiss, and Laura A. Brooks<sup>a)</sup>

*Scripps Institution of Oceanography, La Jolla, California 92093-0238*

*jtraer@ucsd.edu, gerstoft@scsd.edu, peter@coast.ucsd.edu, whodgkiss@ucsd.edu, lbrook02@gmail.com*

**Abstract:** Land-based seismic observations of double frequency (DF) microseisms generated during tropical storms Ernesto and Florence are dominated by signals in the 0.15–0.5 Hz band. In contrast, data from sea floor hydrophones in shallow water (70 m depth, 130 km off the New Jersey coast) show dominant signals in the ocean gravity-wave frequency band, 0.02–0.18 Hz, and low amplitudes from 0.18 to 0.3 Hz, suggesting significant opposing wave components necessary for DF microseism generation were negligible at the site. Florence produced large waves over deep water while Ernesto only generated waves in coastal regions, yet both storms produced similar spectra. This suggests near-coastal shallow water as the dominant region for observed microseism generation.

© 2008 Acoustical Society of America

PACS numbers: 43.30.Nb, 43.30.Pc, 91.30.Ye [WC]

Date Received: April 1, 2008 Date Accepted: June 19, 2008

## 1. Introduction

Microseisms are ubiquitous seismic signals generated by ocean waves.<sup>1</sup> The peak of the microseism spectrum occurs near twice that of ocean surface waves [double frequency (DF) microseisms], generated by the interaction of opposing surface waves of nearly the same wave number.<sup>2</sup> Unlike traveling ocean waves which decay exponentially with depth, the amplitude of the DF pressure pulse does not decay appreciably with depth.<sup>2</sup> Primary microseisms are observed at ocean wave frequencies and are generated only in shallow water by breaking waves or interaction with the sloping bottom.<sup>3</sup> The results from beamforming with seismic arrays suggests that the dominant source regions for primary and double frequency signals may differ in space and/or time.<sup>4</sup>

Recent work suggests that microseisms are only generated when surface waves approach coastal areas<sup>5–8</sup> and that the generation of microseisms is well correlated with ocean surface conditions.<sup>5,9</sup> Storms over the ocean generate large waves causing elevated microseism levels that have been attributed to specific storm events.<sup>4,10</sup>

The surface gravity-wave induced pressure at the sea floor is<sup>5</sup>

$$p = \frac{p_0}{\cosh kH}, \quad (1)$$

where  $p_0$  is the pressure at the surface,  $H$ -ocean depth, and  $k$  the wave number, determined by the surface gravity wave dispersion,  $\omega^2 = gk \tanh kH$ , where  $\omega$  is the angular frequency,  $\omega = 2\pi f$ , with  $f$  the surface wave frequency. For example, with  $H=70$  m (as in the experiment discussed), the pressure from a 0.1 Hz wave will be  $p=0.1p_0$  and the pressure from a 0.3 Hz wave will be  $p=10^{-11}p_0$ . This indicates that the decay of wave pressure with depth is strongly dependent on the wave frequency, and that the pressure spectrum from overhead wave activity observed at the bottom in a shallow-water environment will be dominated by direct forcing

<sup>a)</sup>Also at the School of Mechanical Engineering, University of Adelaide, Adelaide, Australia.

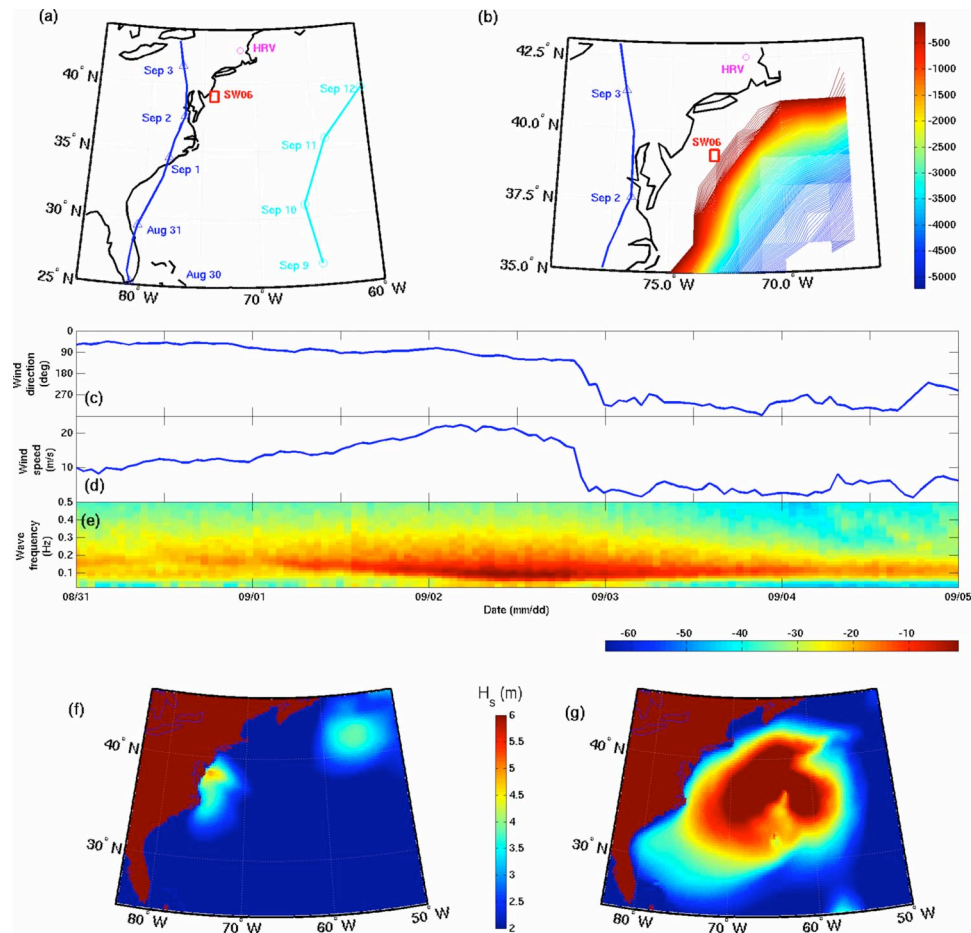


Fig. 1. (Color online) The experiment environment. (a) Experiment location (rectangles) and the recorded path of the storm centers. Triangles mark the storm center for Ernesto and circles the center for Florence every 24 h starting 0 Z 30 August and 9 September, respectively. (b) Bathymetry contours from 100 to 5000 m depth. Water depth less than 100 m is white. (c) Wind direction. (d) Wind speed. (e) The surface wave spectra (dB) from 0.02 to 0.5 Hz for 30 August–3 September. The wave spectral energy is normalized with respect to the highest observed signal. Wind and wave data from the ASIS buoys are averaged over  $\frac{1}{2}$  h periods. (f), (g) Significant wave heights ( $H_s$ ) from Ernesto (9 Z 2 September) and Florence (9 Z 12 September), respectively.

from low frequencies. DF pressure fluctuations will become dominant in deep water because they do not decay appreciably with depth regardless of their frequency.

An opportunity to study storm-generated microseisms on both the ocean bottom and land occurred when waves generated by Tropical Storms Ernesto and Florence passed over the Shallow Water Experiment 2006 (SW06) site during September 2006. Sea floor hydrophones from the SWAMI32, SWAMI52, and SHARK arrays measured pressure variations at the ocean bottom on the shallow-water continental shelf. These were compared with broadband seismic data from the HRV (Harvard) station in Massachusetts.

## 2. Array environment

The edge of the leading right-hand quadrant of Tropical Storm Ernesto passed over the arrays on 2 September, while the inland storm center moved northward [Fig. 1(a)]. The storm, recorded by University of Miami Air-Sea Interaction Spar (ASIS) Buoys,<sup>11</sup> generated steady high winds and wave energy [see Figs. 1(c)–1(e)] over the arrays for 2 days. The wind speed sud-

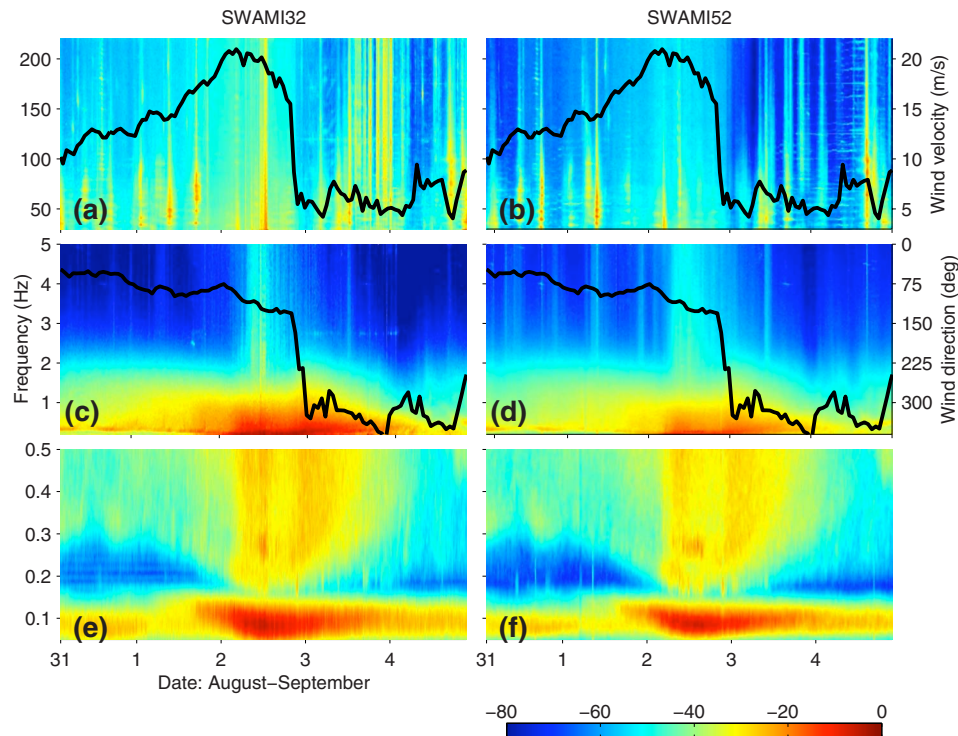


Fig. 2. (Color online) Normalized spectrograms (dB) of the acoustic data at three frequency scales [(a), (b) 30–220 Hz, (c), (d) 0.2–5 Hz, and (e), (f) 0.02–0.5 Hz] obtained over a 5 day period (31 August–4 September) from the SWAMI32 [(a), (c), and (e)] and SWAMI52 [(b), (d), and (f)] arrays. The wind velocity trace from Fig. 1(d) is superimposed in (a) and (b) and the wind direction from Fig. 1(c) is superimposed in (c) and (d). The spectrograms are averaged over five hydrophones and normalized with respect to the highest power spectral density in the observed range.

denly dropped and changed direction near the end of 2 September as the storm passed the arrays [Figs. 1(c) and 1(d)]. Throughout 1 and 2 September the winds blew from the east with speeds from 10 to 20 m/s. From 20 Zulu (20 Z) 2 to 3 September the winds blew from the west at speeds from 2 to 10 m/s. Wave energy remained strong for a further 28 h after the wind dropped [Fig. 1(e)]. The waves underwent a change in direction over 2 September (not shown), transitioning from eastward to south-west incidence, potentially producing an opposing wave field for standing wave generation and transmission of microseisms to the seabed.<sup>2</sup> NOAA hindcasts<sup>12</sup> showed that Ernesto produced large waves in shallow water such as the SW06 site, but not in deep waters [Fig. 1(f)]. The large waves in Fig. 1(f) at (42°N, 55°W) were from another storm. Wave data from the ASIS buoy were consistent with the hindcast results at the site.

On 10 September, large waves from Tropical Storm Florence arrived at the site. Florence moved northward through the Atlantic Ocean with the storm center remaining in deep water [Figs. 1(a) and 1(g)]. The ASIS buoys and both SWAMI arrays were removed prior to the arrival of Florence and no wind or wave data were available. The SHARK array recorded acoustic data through 14 September. The SWAMI and SHARK arrays were situated on a sandy floor at a depth of 70–80 m, 20 km west of the continental shelf and 130 km from the New Jersey coast [Fig. 1(b)].

Although the hydrophones were not designed to work at frequencies less than 2 Hz, the relative spectrogram levels (Fig. 2) were corrected using the SWAMI hydrophone frequency response and the characteristics of the electronic filters. From 10 to 15 Z, 2 September, the

SWAMI32 hydrophones recorded broadband clicks likely attributed to motion of the array. This distortion was minimized by excising any segments with an amplitude greater than 4 s.d. of the signal within each 6 min, 24 sec file. For the SHARK array any segment with an amplitude greater than 8 s.d. was excised. The frequency response of the SHARK hydrophones is unknown. The SHARK frequency response was estimated by comparing the spectra obtained by the SHARK and SWAMI52 arrays over the period of time when the two arrays overlapped (18 Z 25 August to 17 Z 6 September) and assuming the two arrays are measuring the same signal.

### 3. Acoustic spectrograms

At frequencies above 30 Hz, the acoustic levels are well correlated with the local wind speed, while below 2 Hz a significant signal is observed for 2 days after the passing of the storm [Figs. 2(a)–2(d)]. This suggests the signals observed above 30 Hz are generated by wind-induced breaking waves, in agreement with others,<sup>13</sup> and signals below 2 Hz are generated by surface waves. Wave–wave interactions can produce signals as high as 7 Hz,<sup>14</sup> and may be the source of the large signals on 2 September from 2 to 5 Hz.

The signals recorded by the two arrays are similar at frequencies below 2 Hz, suggesting that either these signals travel over the 23 km distance separating the arrays, or that the surface wave spectra are similar over many kilometers. The dominant signal occurred at 0.02–0.18 Hz [Figs. 2(e) and 2(f)] throughout the 5-day period, corresponding to the surface wave frequency band [Fig. 1(e)]. This 0.02–0.18 Hz signal is at a maximum when the storm is above the array. Seismic arrays in California detected a strong 0.07–0.11 Hz signal at this time, originating along an azimuth consistent with the signal being generated in coastal waters between 38 and 40°N.<sup>4</sup> This region includes the SWAMI and SHARK arrays. The peak in seismic signal at this time is not correlated with an increase in wave amplitudes, suggesting that microseism generation may be dependent on the location of the waves. Near these times, NOAA hindcasts show large waves impacting the coast of Cape Cod,<sup>12</sup> which has previously been identified as a site of strong microseism generation.<sup>10</sup>

Relatively low spectral levels were observed in the 0.14–0.18 Hz band during times when the peak in wave energy near 0.08 Hz occurred. The frequency range of the low energy band should include high amplitude DF microseism signals. The ASIS buoy measured the dominant wave direction as westward over 1 September and northward over 2 September, toward the coasts of New Jersey and Cape Cod, respectively. Conceptually, opposing waves from coastal reflection interacting with incoming swells should produce standing waves, however, no DFs were observed at magnitudes equivalent to the primary pressure wave. The absence of DF signal associated with the dominant wave frequency indicates that little opposing wave energy was present. Note that DF microseisms on land and in the deep ocean typically have much higher amplitudes than primary microseisms.<sup>5,10,14</sup> DF levels at HRV are much higher than associated primaries during Ernesto, but the opposite is true at the sea floor arrays, indicating that the signal observed by the arrays is dominated by direct pressure from overhead waves, not from microseisms.

The 0.2–2 Hz signal is 20–30 dB weaker than the 0.02–0.18 Hz signal. It does not appear in the wave spectra, which suggests that this signal is likely either DF microseisms, or due to an inaccurate response of the wave buoy at higher frequencies. The signal maximum in this 0.2–2 Hz band occurs at 03 Z 2 September [Figs. 2(c)–2(f)]. A second signal maxima is observed between 0.2 and 2 Hz at 18 Z 2 September and corresponds to a shift in local wind direction [Figs. 2(c) and 2(d)], suggesting that opposing seas forcing necessary for the DF mechanism occurred.

The SHARK array was used to compute spectrograms from 25 August to 14 September [Fig. 3(b)]. As with the SWAMI measurements of Ernesto, during Florence the dominant signal occurred between 0.02 and 0.18 Hz, corresponding to the dominant wave frequency band, with little signal observed in the associated DF band. As Florence did not make landfall, it had a much larger fetch than Ernesto and produced lower frequency ocean waves for a longer time. The lack of DF signals during both tropical storms suggests that opposing wave compo-

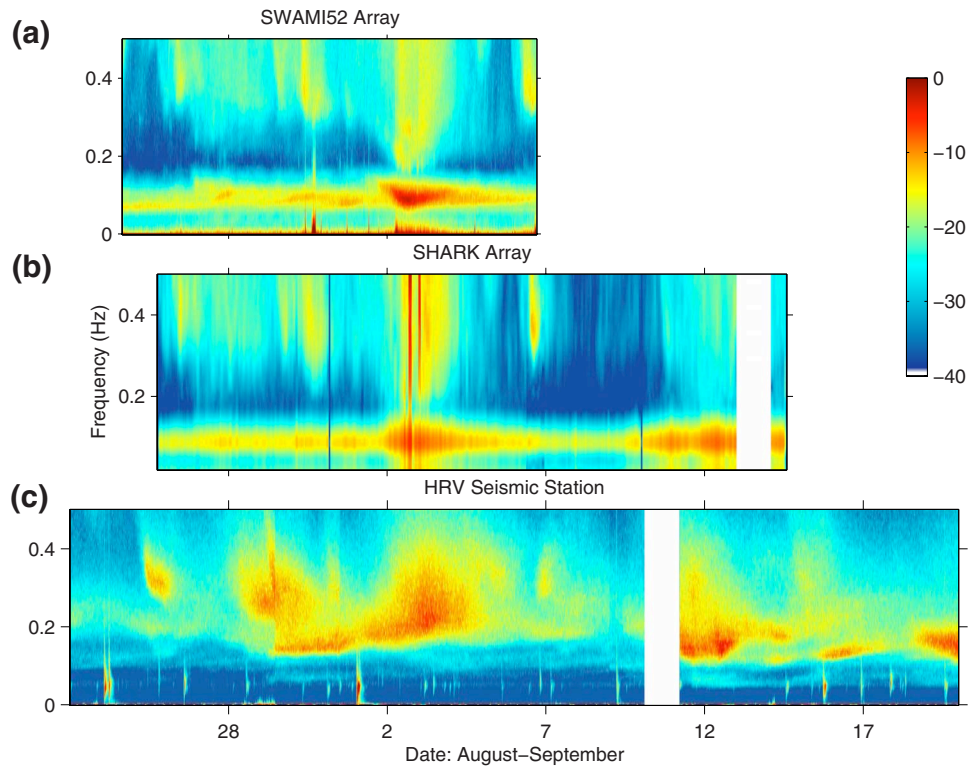


Fig. 3. (Color online) Normalized spectrograms (dB) of the acoustic data between 0.01 and 0.5 Hz from the (a) SWAMI52 array, (b) SHARK array, and (c) HRV seismic station. SWAMI52 data were available from 24 August to 6 September, SHARK data from 25 August to 19 September, and HRV data from 23 August to 20 September.

nents at swell frequencies are not generated by wave reflection/scattering at the coastline nearest the arrays and/or because these components are dissipated by bottom interaction when crossing the relatively wide shallow shelf.

#### 4. Seismic spectrograms

In contrast to the spectrograms from the acoustic arrays, the land-based seismic spectra at HRV are dominated by DF signals between 0.15 and 0.5 Hz, which are 20 dB stronger than the primary signal [Fig. 3(c)]. The microseisms from Ernesto's waves are initially seen at 0.15 Hz on 29 August as Ernesto impacts Florida. The signals are present for 6 days as Ernesto travels northward, increasing in frequency as the storm center moves on land and the fetch of the storm decreases, generating more short period wave energy near shore. The 0.2–0.4 Hz signal present from 29 to 30 August is likely due to a smaller storm to the northeast [Fig. 1(f)]. During the period when Ernesto was over the arrays (2 September), the 0.02–0.18 Hz band that dominated the SWAMI array data was largely absent at HRV, confirming that the signals in that band at the arrays were dominated by direct pressure from overhead waves.

After Ernesto dissipated, another strong set of signals appear from 12 to 14 September, attributed to waves generated by Tropical Storm Florence. The signal from Florence has higher amplitude than that of Ernesto and lower frequency, consistent with the larger waves and fetch of Florence [Figs. 1(f) and 1(g)]. These waves impacted the coasts from Florida to Nova Scotia. As with the seismic signal from Ernesto, the DF signal at HRV from Florence is 20 dB stronger than the primary signal.

## 5. Discussion

The seismic signals of both storms recorded on land were dominated by the DF signals, which is consistent with previous studies and implies that both storms generate DF waves. However, the acoustic levels of Ernesto and Florence contained a weak signal in the lower part of the DF range (0.18–0.25 Hz). Rather, they are dominated by signals at the same frequency as the ocean waves, consistent with a linear forcing mechanism. Despite both storms producing westward traveling waves, no evidence of a wave–wave interaction due to reflection of waves from the coast was observed. This suggests that low frequency opposing waves and corresponding DF microseisms are negligible near the SW06 site, consistent with observations at HRV during the 1991 “Perfect Storm”<sup>10</sup> and that the DF signals detected by the HRV seismic station were generated elsewhere.

When Ernesto reached the SW06 site, the storm center was inland [Fig. 1(f)] and most of the storm-generated waves were in shallow waters. Ernesto produced a significant DF signal at nearby seismic stations over a much longer period of time than the larger storm Florence, which produced larger waves over a greater area in the deep ocean [Fig. 1(g)]. Babcock *et al.*<sup>9</sup> observed high amplitude DF microseisms with an ocean bottom array at a nearby deep water site, indicating that even smaller storms can generate appreciable DF energy and that waves from Florence and Ernesto were likely generating DF microseisms offshore in the open ocean. Despite these large disparities in the size of storms Florence and Ernesto [Figs. 1(f) and 1(g)] the associated microseism signals were similar [Fig. 3(c)], suggesting only near-shore waves produce the signals detected at the HRV seismic station.

The absence of DF signals at the SW06 site may be due to variations in local bathymetry. The SW06 site is separated from the nearest coast by 130 km of shallow water. Waves below 0.1 Hz interact with the bottom at this depth and may attenuate before reaching the coast. It may be the case that the DF microseisms observed at the HRV seismic station are generated in waters shallower than the SW06 site (70 m). The continental shelf narrows substantially near Cape Hatteras to the south and Cape Cod to the north. These regions may be sites of high microseism generation as low frequency waves may attenuate less and hit the coast with more energy.

## Acknowledgments

This project was funded by: the Office of Naval Research, the Department of Energy National Energy Technology Laboratory via the Gulf of Mexico Hydrates Research Consortium, University of Mississippi, and the California Department of Boating and Waterways (to P.D.B.). Data assistance provided by Neil Williams and Hans Graber, University of Miami (local wind and wave data); Arthur Newhall, Woods Hole Oceanographic Institute (SHARK); and Applied Research Laboratories, University of Texas (SWAMI) are appreciated.

## References and links

- <sup>1</sup>S. C. Webb, “The Earth’s ‘hum’ is driven by ocean waves over the continental shelves,” *Nature (London)* **445**, 754–756 (2006).
- <sup>2</sup>M. S. Longuet-Higgins, “A theory of the origin of microseisms,” *Philos. Trans. R. Soc. London* **293**, 1–35 (1950).
- <sup>3</sup>K. Hasselmann, “A statistical analysis of the generation of microseisms,” *Rev. Geophys.* **1**, 177–210 (1963).
- <sup>4</sup>P. Gerstoft and T. Tanimoto, “A year of microseisms in southern California,” *Geophys. Res. Lett.* **34**, L20304 (2007).
- <sup>5</sup>P. D. Bromirski and F. K. Duennebier, “The near-coastal microseism spectrum: Spatial and temporal wave climate relationships,” *J. Geophys. Res.* **107**, 2166 (2002).
- <sup>6</sup>A. Friedrich, F. Krüger, and K. Klinge, “Ocean-generated microseismic noise located with the Gräfenberg array,” *J. Seismol.* **2**, 47–64 (1998).
- <sup>7</sup>T. Tanimoto, “Excitation of microseisms,” *Geophys. Res. Lett.* **34**, L05308 (2007).
- <sup>8</sup>P. Gerstoft, M. C. Fehler, and K. G. Sabra, “When Katrina hit California,” *Geophys. Res. Lett.* **33**, L17308 (2006).
- <sup>9</sup>J. M. Babcock, B. A. Kirkendall, and J. A. Orcutt, “Relationships between ocean bottom noise and the environment,” *Bull. Seismol. Soc. Am.* **84**, 1991–2007 (1994).
- <sup>10</sup>P. D. Bromirski, “Vibrations from the perfect storm,” *Geochem., Geophys., Geosyst.* **2**, 000119 (2001).
- <sup>11</sup>H. C. Graber, E. A. Terray, M. A. Donelan, W. M. Drennan, J. C. Van Leer, and D. B. Peters, “ASIS—A new

- air-sea interaction spar buoy: Design and performance at sea,” *J. Atmos. Ocean. Technol.* **17**, 708–720 (2000).
- <sup>12</sup>“NOAA wavewatch III,” URL [http://polar.ncep.noaa.gov/waves/nww3\\_hist.html](http://polar.ncep.noaa.gov/waves/nww3_hist.html), National Oceanic and Atmospheric Administration, downloaded 20 March 2008.
- <sup>13</sup>D. P. Knobles, S. Joshi, and R. D. Gaul, “Analysis of wind-driven ambient noise in a shallow water environment with a sandy seabed,” *J. Acoust. Soc. Am.* **124**, EL157–EL162 (1993).
- <sup>14</sup>C. S. McCreery, F. K. Duennebier, and G. H. Sutton, “Correlation of deep ocean noise (0.4–30 Hz) with wind, and the Holu Spectrum—A worldwide constant,” *J. Acoust. Soc. Am.* **93**, 2639–2648 (1993).